Communication

An All-Optical Microwave Frequency Divider with Tunable Division Factors Based on DP-DPMZM

Kunpeng Zhai [1,2,†]**, Xuhua Cao** [1,2,†]**, Sha Zhu** [3,*]**, Huashun Wen** [1,*]**, Yinfang Chen** [1]**, Ya Jin** [1,2]**, Xinyan Zhang** [1,2]**, Wei Chen** [1]**, Jiabin Cui** [4] **and Ninghua Zhu** [1]

[1] State Key Laboratory of Integrated Optoelectronics, Institute of Semiconductors, Chinese Academy of Sciences, Beijing 100083, China

[2] University of Chinese Academy of Sciences, Beijing 100049, China

[3] College of Microelectronics, Faculty of Information Technology, Beijing University of Technology, Beijing 100124, China

[4] State Key Laboratory of Information Photonics and Optical Communications, School of Information and Communication Engineering, Beijing University of Posts and Telecommunications, Beijing 100876, China

[*] Correspondence: zhusha@bjut.edu.cn (S.Z.); whs@semi.ac.cn (H.W.)

[†] These authors contributed equally to this work.

Abstract: Based on a dual-polarization dual-parallel Mach–Zehnder modulator (DP-DPMZM), an all-optical frequency divider is proposed and experimentally demonstrated. Two radio frequency (RF) signals are modulated on an optical carrier to work as a dual-beam master laser (ML). The optical signals of the ML are injected into a distributed feedback (DFB) laser to initiate the period-two (P2) state oscillation. By beating the output of the slave laser (SL) via circulator in a photodetector, a frequency divider with tunable factors can be achieved. The innovation of the scheme lies in having a simple structure and only requires optical devices, which is operated in wide RF frequency range without any electrical amplifiers before the photodetector to increase the conversion gain. Experiment results also demonstrate that the frequency division factors can be adjusted.

Keywords: optically injected semiconductor laser; dual-beam injection; microwave photonics; microwave frequency diver

1. Introduction

Frequency dividers are of great importance in radio astronomy, clock comparison and signal processing [1,2] because they can be widely used in generating millimeter waves or frequency synchronization. In radar systems, it is necessary to mix the received high-frequency echo signal with the local oscillator (LO) signal to realize frequency down conversion, so that low-speed electrical devices can be used for signal post-processing. In practical applications, instead of directly using an electrical signal generator to generate low-frequency signals, we need to process the received high-frequency signals to obtain low-frequency signals. Traditionally, frequency dividers include digital or analog types [3]. In contrast to several typical structures of the frequency dividers, they have a high operating band and low power consumption and serve as the first stage of high-frequency dividing. However, all these structures have limited bandwidth because of the bandwidth restrictions of electric filters. Previous designs have faced conflicts between achieving a high operating band and a wide locking range. Thanks to the advantages of microwave photonics, various photonic-based dividers are implemented using a regenerative technique or an injection-locking technique in an optoelectronic oscillator (OEO) loop. For a typical divider system, an OEO loop requires a number of optical and electrical components such as an electrical amplifier and electrical power splitter. For instance, by incorporating a frequency mixer and an optical filter, the frequency division factor can be tuned [4]. Furthermore, a Mach–Zehnder modulator (MZM) operated at the carrier suppression point was used to prevent

OEO free-running oscillation [5]. The method in [6] employed an optical filter and a dual-parallel Mach–Zehnder modulator (DPMZM) to achieve tuning the frequency division factor by adjusting the delay of the OEO loop. Some other methods based on Fourier domain mode-locking [7] were proposed to achieve half-division of frequency.

All-optical microwave frequency dividers based on optical injection [8,9] were proposed to obtain different frequency-division factors, which can be implemented by harnessing the nonlinear dynamics of the semiconductor lasers. These reported techniques rely on direct modulation, which are limited by the low speed of carrier migration in the devices. To overcome this problem, a MZM operated by a radio frequency (RF) is used to generate dual beams which are injected into a distributed feedback (DFB) laser to realize a 1/2 frequency component [10]. However, none of these methods can realize a tunable frequency-division factor.

In this paper, we present a simple integrable and compact all-optical microwave divider with a tunable frequency-division factor. Theoretically, it can be designed with a high-operating frequency because it does not require any electrical amplifiers. By controlling the direct current (DC) bias voltage of the dual-polarization dual-parallel Mach–Zehnder modulator (DP-DPMZM) at a specific point to generate an RF-modulated optical signal for injection of a DFB laser to stimulate period-two (P2) oscillation, a frequency divider can be experimentally achieved. Two RF sources are used to realize a tunable frequency-division factor, and the power of the DFB is sensitive for the P2 station in our scheme. Owing to the frequency-tunable master laser, the dual-beam injection of P2 dynamics can be achieved.

2. Principle

The schematic diagram of the proposed all-optical frequency divider is shown in Figure 1. A continuous tunable laser with a carrier frequency f_c is fed into the DP-DPMZM, which is divided into two paths. The DP-DPMZM in the upper path consists of two orthogonally polarized dual-parallel Mach–Zehnder modulators (DPMZM). The *x*-DPMZM consists of sub-MZM1 and sub-MZM2, which are driven by RF_1 with the connect of a 90° hybrid. The *y*-DPMZM consists of sub-MZM3 and sub-MZM4, which are driven by RF_2 with the connect of another 90° hybrid. By biasing all four sub-MZMs at minimum transmission points, and we set the main DC biases of the DPMZMs at quadrature transmission points, and carrier-suppressed singe sideband (CS-SSB) modulated optical signals are generated. The DP-DPMZM can adjust the frequency division factor by changing RF_1 and RF_2 signals, respectively, to realize a carrier-suppressed single sideband. The optical field at the output of *x*-DPMZM is given by [11].

$$
\begin{aligned}
E_x(t) &\propto E_{MZM1} + E_{MZM2}e^{j\phi_x} \\
&\propto \tfrac{1}{8}E_0 e^{j\omega_0 t}\left[e^{j\beta_{RF1}\sin\omega_{RF1}t} + e^{-j\beta_{RF1}\sin\omega_{RF1}t+j\pi} + \left(e^{j\beta_{RF1}\cos\omega_{RF1}t} + e^{-j\beta_{RF1}\cos\omega_{RF1}t+j\pi}\right)e^{j\phi_x}\right] \\
&\propto \tfrac{1}{4}E_0 e^{j\omega_0 t}\left\{ \begin{array}{l} J_1(\beta_{RF1})e^{j\omega_{RF1}t} - J_1(\beta_{RF1})e^{-j\omega_{RF1}t} + \\ \left[J_1(\beta_{RF1})e^{j\omega_{RF1}t+\frac{\pi}{2}} + J_1(\beta_{RF1})e^{-j\omega_{RF1}t+\frac{\pi}{2}}\right]e^{j\phi_x} \end{array}\right\}
\end{aligned} \tag{1}
$$

where ω_0 and E_0 are the angular frequency and amplitude of the optical carrier. ω_{RF1} is the angular frequency of the RF_1 signal, $\beta_{RF1} = \pi V_{RF1}/V_\pi$ is the modulation index corresponding to RF_2 loaded on the sub-MZMs, V_π is the half-wave voltage of the sub-MZMs, J_0 and J_1 are the zeroth- and first-order Bessel functions of the first kind, ϕ_x is the phase shift introduced by main DC bias of the *x*-DPMZM.

Similarly, sub-MZM3 and sub-MZM4 are driven by the RF_2 signal in the CS-SSB station, the optical field at the output of *y*-DPMZM is given by [11].

$$
\begin{aligned}
E_y(t) &\propto E_{MZM3} + E_{MZM4}e^{j\phi_y} \\
&\propto \tfrac{1}{8}E_0 e^{j\omega_0 t}\left[e^{j\beta_{RF2}\sin\omega_{RF2}t} + e^{-j\beta_{RF2}\sin\omega_{RF2}t+j\pi} + \left(e^{j\beta_{RF2}\cos\omega_{RF2}t} + e^{-j\beta_{RF2}\cos\omega_{RF2}t+j\pi}\right)e^{j\phi_y}\right] \\
&\propto \tfrac{1}{4}E_0 e^{j\omega_0 t}\left\{ \begin{array}{l} J_1(\beta_{RF2})e^{j\omega_{RF2}t} - J_1(\beta_{RF2})e^{-j\omega_{RF2}t} + \\ \left[J_1(\beta_{RF2})e^{j\omega_{RF2}t+\frac{\pi}{2}} + J_1(\beta_{RF2})e^{-j\omega_{RF2}t+\frac{\pi}{2}}\right]e^{j\phi_y} \end{array}\right\}
\end{aligned} \tag{2}
$$

where ω_0 and E_0 are the angular frequency and amplitude of the optical carrier, ω_{RF2} is the angular frequency of the RF_2 signal, $\beta_{RF2} = \pi V_{RF2}/V_\pi$ is the modulation index corresponding to RF_2 loaded on the sub-MZMs, ϕ_y is the phase shift introduced by main DC bias of the y-DPMZM.

Afterwards, two orthogonally polarized signals are combined by a polarization beam combiner (PBC) and amplified by an erbium-doped fiber amplifier (EDFA). By tuning the state of the polarization controller (PC), the optical field of the DP-DPMZM is expressed as

$$\begin{aligned}
E(t) &\propto \cos(\alpha)E_x(t) + \sin(\alpha)E_y(t)e^{j\varphi_{PC}} \\
&\propto \frac{1}{2}E_0\left[J_1(\beta_{RF1})e^{(j\omega_0 t + j\omega_{RF1}t)} + J_1(\beta_{RF2})e^{(j\omega_0 t + j\omega_{RF2}t)}\right]
\end{aligned} \tag{3}$$

where α is the angle between the axial direction of the polarizer and the principal axis of the PBC, and φ_{PC} is the PC-introduced phase shift between the two orthogonal polarization states. The RF_1 and RF_2 modulated optical signal are referred to as an injection light wave from a master laser (ML). The dual-beam is injected into the DFB slave laser (SL) by an optical circulator. The SL has a free running frequency f_s, which is between the dual-beam of the ML as shown in Figure 2.
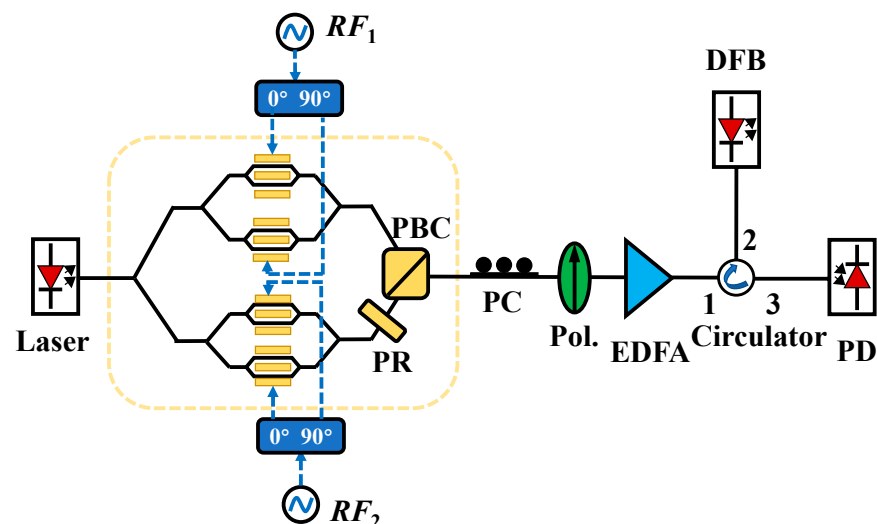

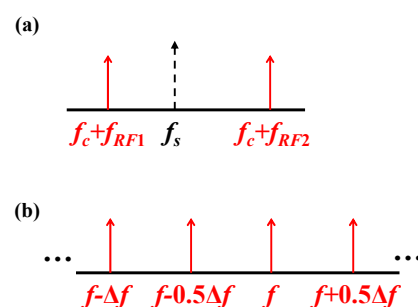**Figure 1.** Scheme of proposed all-optical microwave frequency divider.

Figure 2. (**a**) Optical frequency of the ML and the SL. (**b**) Optical frequency of the SL in P2.

For dual-beam optical injection locking of a semiconductor, the competitions of dynamics have been studied and analyzed [12]. Three general scenarios are shown during injecting a dual-beam from the ML into the SL, including stable locking, periodic oscillation, and chaos. There are two factors affecting nonlinear dynamic states in semiconductors, which is the injection strength ξ and the detuning frequency f_i. The ξ means the amplitude ratio between the ML and the SL. The f_i means the two injections beams frequencies offset from the ML. The SL is interacted with the dual-beam of the ML. Due to the modulation of

the DP-DPMZM, the dual-beam frequencies of the ML can be adjusted by changing the RF_1 and RF_2 signals. This process will cause various nonlinear dynamic states, depending on the control of ζ and f_i. When the period-two (P2) dynamics are achieved, the output frequency spectrum of the SL consists of $f_{M1} - n\Delta f/2$, $f_{M1} + \Delta f/2$ and $f_{M2} + n\Delta f/2$, where n is non-negative integer, f_{M1} and f_{M2} are frequency components of the two ML beams, then the frequency separation $\Delta f = f_{RF1} - f_{RF2}$ is the subtraction of the RF_1 and RF_2 signals, and the SL frequency f_s is suppressed.

The dual-beam frequency of the ML is $f_c + f_{RF1}$ and $f_c + f_{RF2}$, as shown in Figure 2a. We define the $f_c + f_{RF1}$ as $f - \Delta f$ and $f_c + f_{RF2}$ as f. The frequency division factor can be defined as the basic signal frequency divided by the obtained signal frequency. Therefore, in the P2 station, as shown in Figure 2b, the frequencies of SL output spectrum are including components at $f \pm n\Delta f/2$. When the RF_1 has been determined, making the DFB oscillating at P2 state, we can obtain any frequency division factor by adjusting RF_2. The output electrical filed of the SL under P2 state can be expressed as

$$E_{SL}(t) \propto \frac{1}{2}E_0(t)e^{j\omega_0 t} \cdot \sum_{n=0}^{\infty} A_{\pm \frac{n}{2}} e^{\pm j(\frac{n}{2}\omega_{\Delta f} t \pm \theta_{\pm \frac{n}{2}})} \tag{4}$$

where $A_{\pm n/2}$ and $\theta_{\pm n/2}$ are the amplitude and phase of the optical frequency at $f \pm n\Delta f/2$. The output of the SL is detected by a photodetector via circulator. In the proposed system, we can change the injection strength to realize P2 state for microwave dividers, other than OEO loop, it does not need any electrical component or optical amplifiers to compensate the loss.

3. Experiment Results

A proof-of-concept experiment was carried out based on the schematic indicated in Figure 1. An optical carrier generated a continuous-wave (CW) from a tunable laser (Yenista Optics TUNIC-T100S-HP). It is coupled with a polarization controller (PC), which was adjusted to keep the polarization axis matching the DP-DPMZM (Fujistu FTM7977HQA). Two RF signals were generated by microwave signal generators. By setting the DC biases, the RF modulated optical signal, which is also regarded as the injection light from the ML, passed through a PC and PBC. After amplified by an EDFA, the optical signal was routed from Port 1 to Port 2 through an optical circulator. The DFB laser connected to Port 2 and the photodetector connected to Port 3 of the circulator.

The wavelength of the free running DFB laser is 1545.35 nm. The frequency components in Figure 3 are the original ML carrier and sidebands and P2 station. The P2 station frequency components are in the middle of the RF modulation sidebands and have different amplitudes. The frequency components close to the DFB laser frequency have higher amplitudes than those away from the DFB laser frequency. In the P2 state of the DFB laser, there are multiple frequency components, which are caused by the resonator in the laser and will not affect the system performance. The ML is modulated by RF signals, and its sidebands are adjustable to make SL wavelength in the middle. The spectrum of the optical signal was measured by the optical spectrum analyzer (OSA, Yokogawa AQ6730D). The resolution of the OSA is 0.02 nm, in which it is difficult to distinguish the RF and LO signals in optical spectra. When the ML is injected into the SL, the resonant state in the DFB cavity will change, with the upper and lower RF modulation sidebands. The frequency divider output spectrum is shown in Figure 3. The optical signal-to-noise ratio (OSNR) is related to the P2 state of optical injection and the input optical power. The optical frequency components contain the ML carrier and sidebands. By adjusting them in the middle of the RF modulation sidebands, they have different amplitudes. The optical signal near the SL frequency has higher optical power and better OSNR. The P2 station of the laser will also affect the OSNR, this is reflected in the influence of laser cavity length on P2 resonance. The DFB laser is operated at 25 °C and its output power is 0.35 dBm.
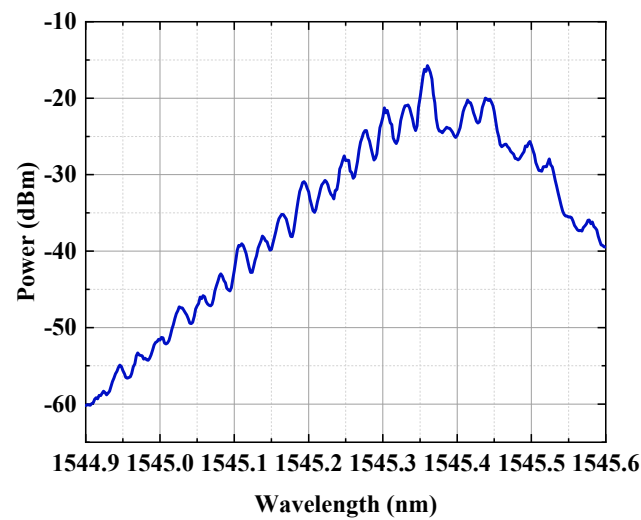
Figure 3. Optical spectrum of the microwave frequency divider.

The electrical spectrum of microwave frequency divider is shown in Figure 4, which is measured with an electrical signal analyzer (ESA). The RF_1 and RF_2 signals are 5 GHz and 11 GHz, respectively. The beams emitted from the SL are captured by the photodetector (PD). The $\Delta f/2$ is 3 GHz, then the 8 GHz frequency component is obtained. This proves that the function of the frequency divider can be realized through an all-optical method. Because the RF signals peak frequency emitted by the two electrical signal generators are different between 5 GHz and 11 GHz, this causes the target signal peak frequency not to be 8 GHz. The power of the 8 GHz frequency component is −38.2 dBm, with the RF signal is 0 dBm, the system has a conversion gain of −38.2 dBm. The full width at half maximum (FWHM) depends on elements of device system, such as the RF signals generated from the electrical signal generators. There are no optical amplifiers before the photodetector, and there are no electrical amplifiers to increase the conversion gain.
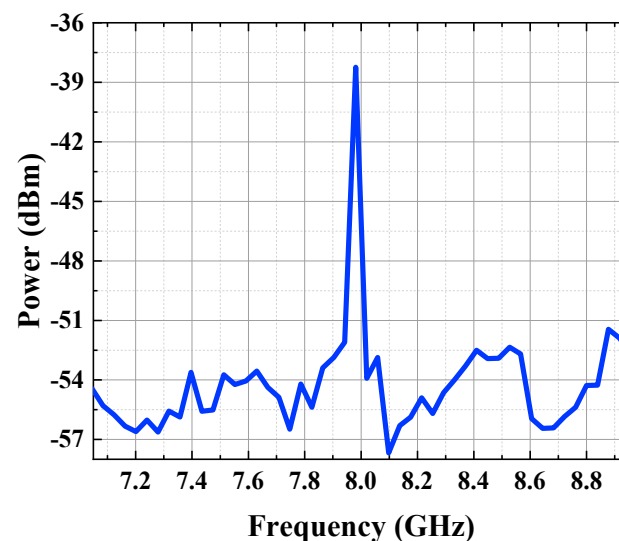

Figure 4. Electrical spectrum of the microwave frequency divider.

Microwave frequency division for different input RF signals was investigated. By changing the RF_1 and RF_2 signals to obtain different $\Delta f/2$, we can obtain tunable frequency-division factors. Table 1 shows the RF signals data in the experiment, f_{target} is the target frequency that we need to obtain. By changing the RF signals, the proposed all-optical frequency divider can realize any division factors, as shown in Figure 5. The frequency divider output electrical spectrum measured on ESA connected to PD. First, we adjust the

RF_2 signal to 11 GHz. By changing the RF_1 signal to 5 GHz and 7 GHz, respectively, we can generate 8 GHz and 9 GHz f_{target} signals. Then the RF_1 signals are set to 5 GHz, 6 GHz and 7 GHz, respectively, and the corresponding RF_2 signals are set to 15 GHz, 14 GHz and 13 GHz, respectively, and the f_{target} values are all 10 GHz. At last, we adjusted RF_1 signal to 7 GHz and RF_2 signal to 15 GHz,17 GHz, so that f_{target} can generate 11 GHz and 12 GHz signals. The frequency component at 8 GHz to 12 GHz can be seen, this verifies the adjustable division factor frequency divider operation.

Table 1. The RF signal data in experiment.

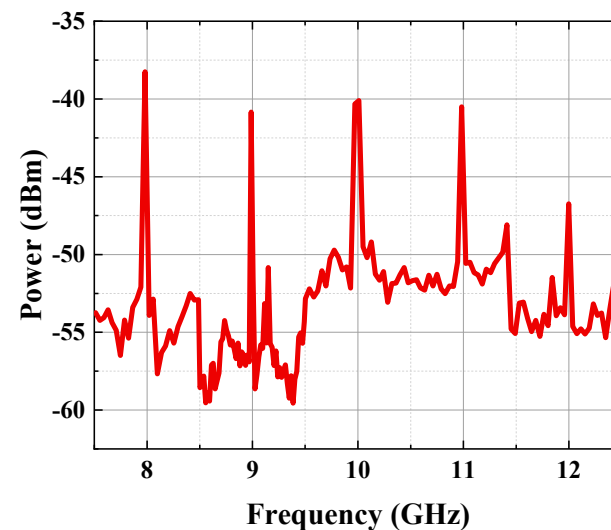| RF_1 (GHz)	RF_2 (GHz)	$\Delta f/2$ (GHz)	f_{target} (GHz)
5	11	3	8
7	11	2	9
5	15	5	10
6	14	4	10
7	13	3	10
7	15	4	11
7	17	5	12

Figure 5. Electrical spectrum of the proposed all-optical microwave frequency divider.

As shown in Figure 6, with the change in RF_1 and RF_2 signals, we keep the f_{target} as 10 GHz. The RF_1 signal is 5 GHz, 6 GHz, 7 GHz, respectively. The RF_2 signal is 15 GHz, 14 GHz, 13 GHz, respectively. The frequency divider corresponding to the change of different RF_1 and RF_2 signals has different frequency division factors, and the final target frequency signal is 10 GHz. The corresponding power of the state noise and frequency peak value under different frequency division factors is different. By controlling the RF signals, the proposed all-optical microwave frequency divider can achieve different frequency division factors. The systems parameters such as optical power and SL frequency can be optimized to extend the signal noise rate (SNR). In Figure 6, the State1 (RF_1 = 5 GHz, RF_2 = 15 GHz) has the SNR over 22 dBm, and the State 2 (RF_1 = 6 GHz, RF_2 = 14 GHz) and the State 3 (RF_1 = 7 GHz, RF_2 = 13 GHz) have the SNR about 18 dBm and 12 dBm, respectively. This is caused by the different RF signals value. For the influence of optical power for oscillation state, the ML power was changed accordingly as the input RF signal frequency value to ensure the SL was in P2 state.
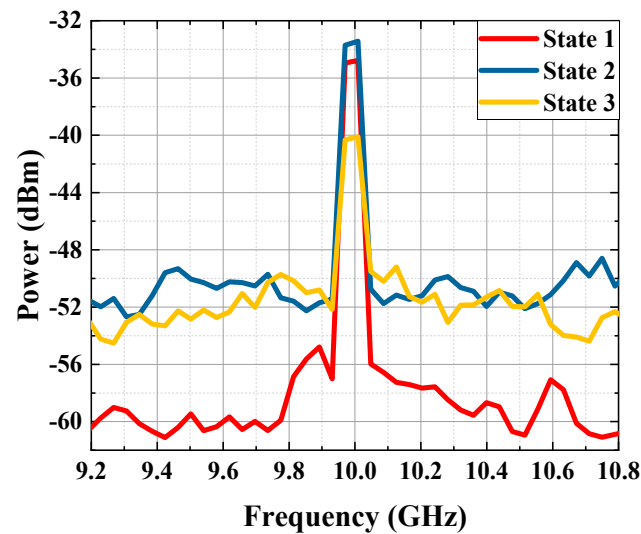
Figure 6. Electrical spectrum of the proposed all-optical microwave frequency divider, with the f_{target} is 10 GHz.

4. Conclusions

A tunable division factors all-optical microwave divider is proposed, and experiment demonstrated. Based on the dual-beam injection effect, the DFB laser is oscillating in a P2 state. With the help of DP-DPMZM, two CS-SSB sidebands are generated to inject in the DFB by driving two RF signals in two orthogonal DPMZM branches. Then the optical frequency component is produced. There is no electrical component and optical or electrical amplifier in the proposed scheme. The power of the 8 GHz frequency component is -38.2 dBm, with the RF signal is 0 dBm, the system has a conversion gain of -38.2 dBm. Experimental results demonstrate that the frequency division factors can be adjusted.

Author Contributions: Conceptualization, K.Z. and X.C.; methodology, K.Z., X.C. and S.Z.; validation, K.Z. and X.C.; formal analysis, K.Z., J.C. and S.Z.; investigation, K.Z., H.W. and Y.C.; resources, S.Z., H.W. and N.Z.; data curation, Y.J., X.Z. and X.C; writing—original draft preparation, K.Z. and S.Z.; writing—review and editing, K.Z. and S.Z.; visualization, K.Z. and S.Z.; supervision, S.Z., H.W., W.C. and N.Z.; project administration, K.Z., S.Z., H.W. and N.Z.; funding acquisition, S.Z., H.W. and N.Z. All authors have read and agreed to the published version of the manuscript.

Institutional Review Board Statement: Not applicable.

Informed Consent Statement: Not applicable.

Data Availability Statement: Not applicable.

Conflicts of Interest: The authors declare no conflict of interest.

References

1. Fortier, T.M.; Kirchner, M.S.; Quinlan, F.; Taylor, J.; Bergquist, J.C.; Rosenband, T.; Lemke, N.; Ludlow, A.; Jiang, Y.; Oates, C.W.; et al. Generation of ultrastable microwaves via optical frequency division. *Nat. Photon.* **2011**, *5*, 425–429. [CrossRef]
2. Li, J.; Yi, X.; Lee, H.; Diddams, S.A.; Vahala, K.J. Electro-optical frequency division and stable microwave synthesis. *Science* **2014**, *345*, 309–313. [CrossRef] [PubMed]
3. Bomford, M. Selection of frequency dividers for microwave PLL applications. *Microw. J.* **1990**, *33*, 159–165.
4. Han, D.; Wei, W.; Liu, Z.; Xie, W.; Dong, Y. Sub-terahertz photonic frequency divider with a large division ratio based on phase locking. *Opt. Lett.* **2021**, *46*, 4268–4271. [CrossRef] [PubMed]
5. Liu, S.; Lv, K.; Fu, J.; Wu, L.; Pan, W.; Pan, S. Wideband microwave frequency division based on an optoelectronic Oscillator. *IEEE Photon. Technol. Lett.* **2019**, *31*, 389–392. [CrossRef]

6. Duan, S.; Mo, B.; Wang, X.; Chan, E.; Feng, X.; Yao, J. Photonic-assisted regenerative microwave frequency divider with a tunable division factor. *J. Light. Technol.* **2020**, *38*, 5509–5516. [CrossRef]
7. Wang, Y.; Li, X.; Wo, J.; Zhang, J.; Wang, A.; Du, P. Photonic frequency division of broadband microwave signal based on a Fourier domain mode-locked optoelectronic oscillator. *Opt. Laser Technol.* **2022**, *147*, 107704. [CrossRef]
8. Fan, L.; Wu, Z.; Deng, T.; Wu, J.; Tang, X.; Chen, J.; Mao, S.; Xia, G. Subharmonic Microwave Modulation Stabilization of Tunable Photonic Microwave Generated by Period-One Nonlinear Dynamics of an Optically Injected Semiconductor Laser. *J. Light. Technol.* **2014**, *32*, 4660–4666. [CrossRef]
9. Zhang, M.; Liu, T.; Wang, A.; Zhang, J.; Wang, Y. All-optical clock frequency divider using Fabry–Perot laser diode based on the dynamical period-one oscillation. *Opt. Commun.* **2011**, *284*, 1289–1294. [CrossRef]
10. Chen, H.; Chan, E.H.W. Ultra-Simple All-Optical microwave frequency divider. *IEEE Photon. Technol. Lett.* **2022**, *34*, 219–222. [CrossRef]
11. Zhang, S.J.; Wang, H.; Zou, X.H.; Zhang, Y.L.; Lu, R.G.; Liu, Y. Calibration-free electrical spectrum analysis for microwave characterization of optical phase modulators using frequency-shifted heterodyning. *IEEE Photon. J.* **2014**, *6*, 5501008.
12. Qi, X.Q.; Liu, J.M. Dynamics scenarios of dual-beam optically injected semiconductor lasers. *IEEE J. Quantum Electron.* **2011**, *47*, 762–769. [CrossRef]